Ind. J. Pharm. Edu. Res., 2025; 59(4):1293-1304.
https://www.ijper.org

Original Article

Co-Delivery of Sphingosomal Formulation Containing BCL2 siRNA Doxorubicin for the Treatment of Lung Cancer

Prashant Nayak, Rompicherla Narayana Charyulu*

Department of Pharmaceutics, NITTE (Deemed to be University), NGSM Institute of Pharmaceutical Sciences, Deralakatte, Mangalore, Karnataka, INDIA.

ABSTRACT

Background: Lung cancer continues to pose a major challenge to global health, with limited therapeutic options and high mortality rates. One factor that contributes to this is the overexpression of BCL2, an anti-apoptotic protein that plays a role in tumor progression and resistance to therapy in lung cancer. To address this challenge, we investigated the potential of a co-delivery strategy using a sphingosomal formulation to simultaneously deliver BCL2 siRNA and Dox, a commonly used chemotherapy drug. **Materials and Methods:** The sphingosomal formulation was prepared using a combination of sphingomyelin and cholesterol, providing stability and controlled release properties. BCL2 siRNA and Dox were incorporated into the sphingosomes within the liposomal core. The formulation was characterized by size, surface charge and encapsulation efficiency. NTA analysis was performed and TEM was done to check surface morphology, MTT, SRB, apoptosis and cell cycle assay for anticancer activity. **Results:** The formulation SD particle size by Malvern zeta sizer was found to be 165.1 nm. In TEM results also the range was in 145-205 nm whereas NTA analysis showed the size of the SD formulation as 173.8 nm hence the particle size of the formulation is in the Nano range of 200 nm. The anti-cancer activity of SD formulation was confirmed by MTT with IC_{50} of 0.285 µm and SRB assay IC_{50} of 0.357 µm against A 549 cell lines. The formulation SD showed very significant anti-cancer activity against Dox. Apoptosis and cell cycle analysis showed the formulation SD was much better in efficacy as compared to Dox. **Conclusion:** The Sphingosomal formulation (SD) effectively co-delivers BCL2 siRNA and Dox, demonstrating superior anti-cancer activity against A549 cell lines compared to Dox alone. The formulation's nanoscale size and enhanced efficacy highlight its potential as a promising strategy to improve treatment outcomes and address resistance in lung cancer.

Keywords: BCL2 siRNA, Doxorubicin, TEM, Lung cancer, MTT.

Correspondence:
Dr. Rompicherla Narayana Charyulu
Department of Pharmaceutics, NITTE (Deemed to be University), NGSM Institute of Pharmaceutical Sciences, Deralakatte, Mangalore-575018, Karnataka, INDIA.
Email: narayana@nitte.edu.in

Received: 27-01-2025;
Revised: 02-04-2025;
Accepted: 19-06-2025.

INTRODUCTION

The public's overall health and well-being face a significant threat from lung cancer, a malignancy that has shown a high incidence and mortality rate in recent years.[1-3] Despite the widespread use of targeted chemotherapy in clinical settings, its effectiveness is limited by challenges such as systemic toxicity, lack of tumour selectivity and the development of Multidrug Resistance (MDR). Combination therapy, involving the simultaneous administration of multiple drugs with different mechanisms of action, has traditionally been the most effective approach to chemotherapy.[4-6] By allowing each drug to be used at its optimal dose without causing severe side effects, this strategy reduces the likelihood of cancer cells developing resistance. Therefore, in cancer research and treatment, combinations of anticancer drugs like carboplatin (Carbo), paclitaxel (Tax) and Dox have been commonly utilized.[7-9]

The gene known as BCL2 (B-Cell Lymphoma 2) is significant in controlling both cell survival and apoptosis (programmed cell death). Abnormal expression of BCL2 has been associated in various cancers, including lung cancer, where it can contribute to tumor growth, resistance to therapy and poor prognosis.[10-14] Induction of apoptosis: Overexpression of BCL2 in cancer cells can protect them from undergoing apoptosis, allowing them to survive and proliferate uncontrollably. By using siRNA to specifically target BCL2 mRNA, it is possible to reduce BCL2 protein levels in cancer cells. This reduction in BCL2 expression can trigger apoptosis, leading to the death of cancer cells.[15-17]

Increased sensitivity to chemotherapy and radiation

Overexpression of BCL2 has been linked to resistance to chemotherapy and radiation therapy in lung cancer. By suppressing BCL2 expression using siRNA, cancer cells may become more vulnerable to the cytotoxic effects of these

DOI: 10.5530/ijper.20257236

treatments. The combination of BCL2 siRNA and conventional therapies may improve their effectiveness and overcome drug resistance.[18]

Synergistic effects with targeted therapies

BCL2 is involved in the regulation of apoptotic pathways and can contribute to resistance to targeted therapies in lung cancer. Combining BCL2 siRNA with targeted therapies, such as EGFR inhibitors or ALK inhibitors, has shown the potential to enhance treatment response and overcome resistance mechanisms. This synergistic approach can improve the effectiveness of targeted therapies in lung cancer treatment.[19] Inhibition of tumour proliferation and spread: BCL2 has been associated with the growth and metastasis of lung cancer cells. By silencing BCL2 expression using siRNA, it may be possible to inhibit tumour growth and metastatic spread. This can be achieved by promoting apoptosis, inhibiting angiogenesis and modulating signalling pathways involved in cancer cell survival and migration.[20,21]

Dox is widely recognized for its ability to combat cancer. It is frequently administered in medical settings to treat different forms of cancer in both adults and children.[22,23] A variety of investigations have associated the anticancer properties of Dox with its ability to insert itself between the DNA molecules within tumor cells, creating DNA cross-links and interacting with proteins convoluted in DNA repetition and transcription, such as topoisomerase II. Moreover, Dox has been observed to produce reactive oxygen species, thereby enhancing its anticancer properties.[24,25] The administration of Dox is hindered by its detrimental impact on the heart, leading to cardiovascular toxicity.[26] Although Dox can affect various organs such as the brain, liver and kidney, it appears that heart is particularly vulnerable its toxic effects.[27] Specifically, acute cardiovascular toxicity is found in approximately 11% of patients are given Dox,[28] whereas chronic myopathy is less common, occurring in roughly 1.7% of cases.[29] Even after significant research efforts over time, the exact mechanism responsible for the cardiovascular toxicity induced by Dox remains uncertain. Various theories have been suggested to elucidate this toxicity, with topoisomerase II, a target affected by Dox, being recognized as a potential contributor to cardiovascular toxicity.[30,31] Dox facilitates oxidative stress through enzymatic pathways and induces the production of hydroxyl radicals. These radicals are responsible for protein alterations, DNA damage, lipid peroxidation and ultimately cell death through or necrosis or apoptosis. This process is the primary cause of Dox-induced cardiovascular toxicity. Regarding cardiovascular toxicity, existing literature suggests that Dox disrupts calcium ions and activates p53-dependent pathways.[32] (Ca^{2+}) handling[33] and triggers cytochrome c-mediated apoptosis by activating caspase 3 and 9.

The literature also highlights that the cardiotoxicity induced by Dox is associated with its interaction with various proteins. Therefore, a potential strategy to reduce the toxic side effects of Dox is to attach it to a large molecule that can prevent the protein-Dox interactions required for triggering Dox toxicity. This conjugate would accumulate in cancer cells and release Dox, enabling it to exert its cytotoxic effects.

The formulation was designed by encapsulating siRNA and Dox within sphingosomal nanoparticles. This approach aims to reduce Dox-induced cardiotoxicity and lower its required dosage, specifically targeting multidrug-resistant cancers.

MATERIALS AND METHODS

Materials

Dox (Yarrow Chemical, Mumbai), Cholesterol (HI media, Mumbai), Sphingomyelin (Sigma Aldrich, Bangalore), siRNA (Takara bio-India Limited, Bangalore). DMEM and Fetal Bovine Serum (HI media, Mumbai).

The formulation of Dox and sphingosomes was designed using the Design of Experiments (DoE) approach. The selection of the Dox and lipid concentrations for the formulation was based on a review of existing literature and optimization was planned using DoE software. 3^2 factorial design was used for the formulation, Table 1 contains the experimental setup and actual values for the independent variables.

Preparation of sphingosome

Sphingosomes containing Dox, soya lecithin and cholesterol were prepared using the thin film hydration method. The components were dissolved in a mixture of chloroform and methanol (9:1 ratio) with specific concentrations mentioned in Table 2. The solution was poured into a round-bottom flask of a rotary flash evaporator and the organic solvent was evaporated at 60°C for 15 min with a rotation speed of 90 rpm. The thin layers formed on the inner surface of the flask were dried overnight in a vacuum oven.

Next, the dried lipid layer was rehydrated with Phosphate-Buffered Saline (PBS) at pH 7.4. The suspension was vortexed for 10 min and then hydrated for 1 hr at 70°C and 90 rpm. The liposomal suspension was then subjected to ultra-centrifugation at 3000 rpm for 30 min. The final formulation was prepared by taking the specified drug ratio and sonicating it for 15 min.

The optimized formulation was analyzed for particle size, Polydispersity Index (PDI) and zeta potential to evaluate its properties.

The assessment of the optimized formulation included the determination of particle size, Polydispersity Index (PDI) and zeta potential parameters using the Zeta Sizer (Malvern, India), UK. The particle size was measured using dynamic light scattering, while the zeta potential was determined using the

same instrument. The measurements were carried out in folded capillary cells and the results were recorded for further analysis.[34]

Entrapment Efficiency (EE)

To calculate the Entrapment Efficiency (EE) of the formulation, a spectrophotometric method was utilized. A specific quantity of Nanoparticulate dispersion was centrifuged at 10,000 RPM for 15 min using a REMI centrifuge (BL-135R). The concentration of the free drug in the supernatant was determined using a spectrophotometer. The EE was then determined by applying the following formula: EE=(Total drug-free drugin EE)/Total drugx100%.[35]

Or, alternatively: Entrapment Efficiency (EE)=(weight of drug added in the formulation - weight of freed drug in EE)/(weight of drug added in the formulation)x100 (Equation 1)

Transmission Electron Microscopy (TEM)

To examine the sample using Transmission Electron Microscopy (TEM), the sample was first diluted with deionized water at a ratio of 1:20 and then subjected to sonication for 3 min before analysis. A carbon-coated copper grid was used to hold a drop of the diluted solution of CLCAE and CLAA separately, forming a liquid film. To negatively stain the film, a drop of ammonium molybdate (2% w/w) in 2% w/v ammonium acetate buffer with a pH of 6.8 was added. After removing excess stain with filter paper, the dried and stained film was observed under a transmission electron microscope to analyze and compare the surface morphology.[36]

Nanoparticle Tracking Analysis (NTA)

NTA was employed to determine the size, concentration and number of particles present in the dispersion. NTA is a real-time, number-based particle-tracking technology that utilizes the principles of both Brownian motion and light scattering to provide information on the concentration of dispersed nanoparticles. The diffusion coefficient of individual particles is measured through NTA, based on the movements of particles captured in successive optical video images. The NTA analysis was conducted using the Malvern NanoSight instrument.

In summary, the liposome samples were appropriately diluted to achieve a particle count of 30 to 60 particles per image frame. The samples were then injected into the sample chamber, where sequential images were captured and measurements were taken in triplicates. These images were subsequently analyzed using the NTA 3.4 software.[37]

Procurement of cell lines and their maintenance

The A549 lung cancer cell lines were obtained from the National Centre for Cell Sciences (NCCS) in Pune. These cells were grown in Dulbecco's Modified Eagle's Medium (DMEM) supplemented with 10% Fetal Bovine Serum (FBS), 20 µg/mL penicillin (100 U) and 100 µg/mL streptomycin. They were regularly sub-cultured and maintained in T25 flasks at 37°C with 5% CO_2 in a humidified incubator until they reached 70% confluence.

To prepare the test samples, a stock concentration of the SD formulation, DXOX and sphingosomes was initially established at a concentration of 10 mg/mL in 5% Dimethyl Sulfoxide (DMSO) in sterile water. This stock solution underwent filtration using a 0.22 µm syringe filter. Various concentrations ranging from 5 to 160 µg/mL were derived from this stock solution for the MTT assay. All experiments were conducted in triplicate to ensure the reliability and reproducibility of the results.

MTT assay

The MTT staining procedure, originally described by and slightly adapted, involved the following steps: Each well of the plate was treated with 20 µL of a 5 mg/mL MTT reagent and then incubated for 24 or 72 hr. Subsequently, the samples were incubated for 4 hr at 37°C. The medium was aspirated and the wells were washed with PBS. Following a drying period of approximately 2 hr, 200 µL of Dimethyl Sulfoxide (DMSO) was added to each well. The microtiter plate was agitated to dissolve the formazan crystals. Measurements were recorded at 570 nm using an ELX800 UV universal microplate reader manufactured by Bio-Tek Instruments Inc. in Vermont, USA, with a reference wavelength set at 630 nm.[38-40]

$$Cell\ viability(\%) = \frac{OD_{treat} - OD_{blank}}{OD_{control} - OD_{blank}} \times 100\%$$

Sulforhodamine B assay (SRB)

The cells were fixed by adding trichloroacetic acid to achieve a final concentration of 10%.[41-43] The plate was then placed in the refrigerator at 4°C for 24 hr. Subsequently, the plate was rinsed with tap water and air-dried for approximately 1 hr. The wells were stained with SRB stain (0.057% in 1% acetic acid) for 30 min. After staining, the plate was washed with 1% acetic acid to remove any excess stain and allowed to dry for around 30 min. To extract the stain, 200 µL of TRIS buffer (10 mM, pH 10.5) was added to each well and the plate was shaken for approximately 30 min. The absorbance was then measured at 540 nm using an ELX800 UV universal microplate reader (Bio-Tek Instruments Inc., Vermont, USA) with a reference wavelength of 630 nm.

$$Cell\ viability(\%) = \frac{OD_{treat} - OD_{blank}}{OD_{control} - OD_{blank}} \times 100\%$$

Flow cytometry

Cell apoptosis was assessed using an Annexin V-FITC/PI apoptosis analysis kit. A549 cells were plated in 6-well plates upon reaching 80% confluence and treated with Dox and the SD formulation. After 72 hr, the cells were harvested by trypsinization, centrifuged, washed with PBS and resuspended in 100 µL of binding buffer. Subsequently, the cells were stained with Annexin V-FITC and Propidium Iodide (PI) and incubated

in the dark for 15 min. Apoptotic cells were then analyzed using a flow cytometer (BD Biosciences, USA).

Cell Cycle Assay

A549 cells were cultured for 24 hr with 1×10^6 cells per well in a 6-well plate. After 24 hr, when attached cells were formed in each well, the medium was replaced with a solution containing the IC_{50} concentration of Dox and SD. Subsequently, cells were harvested from each well, washed twice with PBS and suspended in 300 µL of PBS. Then, 0.7 mL of 100% ethanol was gradually added to the suspension.

The tubes containing the cell suspension were stored at -4°C for at least 1 hr. Following centrifugation, the pelleted cells were treated with 250 µL of 50 mg/mL PI solution and 100 µL of PBS. The tubes were kept in the dark for 1 hr as PI has the capability to bind to DNA and stain cells at different stages of the cell cycle. The labelled cells were then analyzed using a flow cytometer to determine the percentage of cells in each phase of the cell cycle (Applied Bio-system, USA).

RESULTS AND DISCUSSION

Formulation was optimized by DOE software and prepared by thin film hydration method quantity of the optimized formulation used is given in Table 1 the optimized formulation was called SD formulation, The formulation, with a drug-to-lipid ratio of 1:6, was subjected to characterization, including particle size analysis, Polydispersity Index (PDI) and zeta potential measurement.

The particle size of the formulation from Figure 1 was found to be 165.1±2.56 nm, The PDI of the formulation SD was found to be 0.255, Result quality of the formulation was found to be good.

From Table 3 and Figure 2 the zeta potential was -33.4 mV of the SD formulation.

Entrapment Efficiency

The formulation SD exhibited an entrapment efficiency of 75.86%. The free drug/untrapped drug which was collected after centrifugation and UltraViolet absorbance was taken and was substituted from the equation of y= 0.0118x-0.003 which was obtained from the calibration curve of dox. The concentration found was the concentration of the free drug which was substituted in the equation and the final value of the EE of SD formulation was found to be 75.86%.

Transmission electron microscopy (TEM)

Figure 3 illustrates the Transmission Electron Microscopy (TEM) image, showing that the particles in the formulation demonstrated variability in size and were mainly spherical in shape and had smooth surfaced texture. The particle size analysis of the SD formulation indicates that the particles ranged in size from approximately 145-205 nm.

Nanoparticle Tracking Analysis (NTA)

From the results shown in Figure 4 the mean particle size was found to be 173.8 nm D10 was 132.2 nm, D50 was found to be 165.7 nm and D90 was 237.0 nm.

Table 1: 3^2 factorial designs for sphingosome formulations of Dox HCl: coded levels and actual values for each factor.

Factors	Levels, actual (coded)		
	-1 (Low)	0 (Medium)	+1 (High)
Independent variables	1:1	1:2	1:3
A=Dox HCl: sphingosomes (W:W)	10	15	20
B = Sonication time (min)			
Dependent variables	…..	…..	…..
R1=Particle Size (nm) (R1)	…..	…..	…..
R2=PDI	…..	…..	…..
R3=Entrapment efficiency (%) (R2)			

Table 2: Formulation of SD formulation.

Sl. No.	Ingredients	Quantity	Uses
1	Dox	0.01 gm	Anti-cancer drug
2	siRNA	10 µL	Gene silencing
3	Sphingosomes	0.06 g	Lipid bilayer
4	Cholesterol	0.02 g	Stabilizers

Table 3: Zeta potential of formulation SD.

Parameters	Values	Peak	Mean (mV)	Area (%)	Width (mV)
Zeta Potential (mV):	-33.4±2.37	Peak 1:	-31.9	93.0	8.40
Zeta Deviation (mV):	10.2	Peak 2:	-57.1	7.0	4.24
Conductivity (mS/cm):	0.0219	Peak 3:	0.00	0.0	0.00

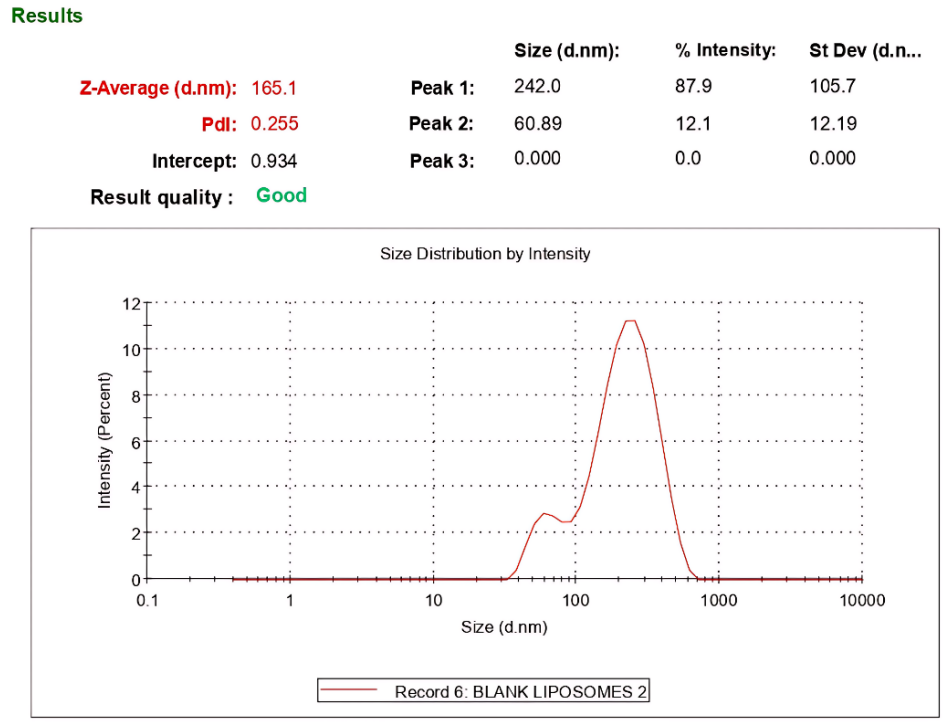

Figure 1: Particle Size, Polydispersity Index (PDI).

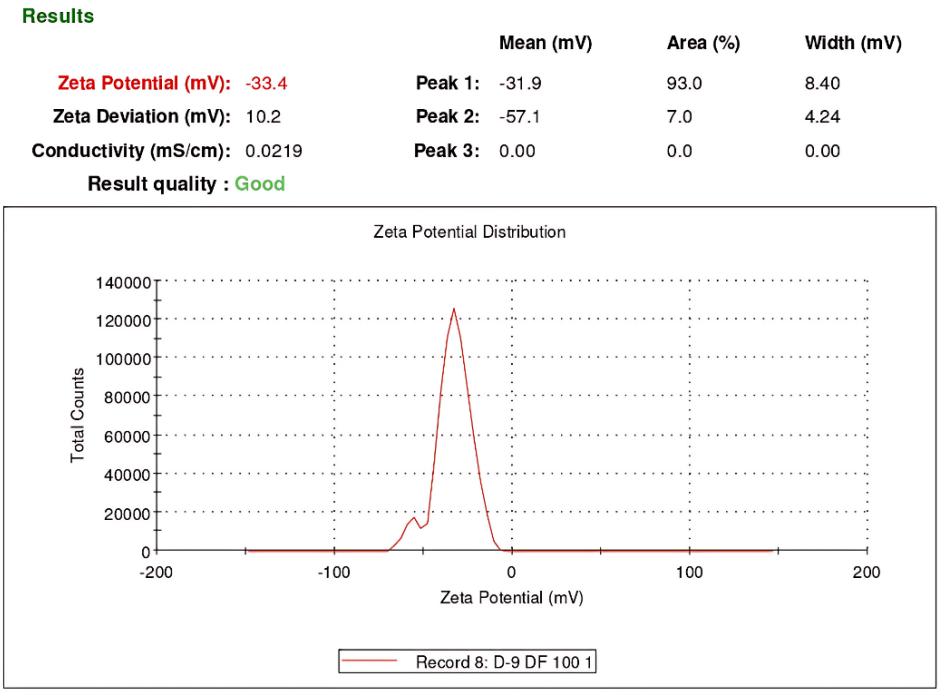

Figure 2: Zeta potential of the formulation SD.

The results is in with the correlation with TEM (145-205 nm), particle size analysis results (165.1 nm) and NTA was 173.8 nm so the results don't show much deviation in particle size of the SD formulation.

MTT assay

As sown in Figure 5 In the MTT assay IC_{50} of the sphingosomes is found to be 2.407 µm Dox is found to be 0.621 µm and formulation SD is found to be 0.285 µm. From this data, the formulation is twice as effective as compared to Dox solution.

Sulforhodamine B assay (SRB)

In the case of SRB assay IC_{50} of the sphingosomes is found to be 2.807 µm and Dox is found to be 0.721 µm and formulation SD is found to be 0.357 µm. From this data the formulation is twice as effective as compared to Dox solution.

Apoptosis analysis

As shown in Figure 6 A and B Dox was found to be 85.49% and in formulation it was found to be 90.88% this show in quadrant 3 formulation of siRNA and Dox sphingosomes were more effective as compared to Dox alone.

Cell Cycle Assay

As show in Figure 7A Dox showed RN1(G1) is 16.86%, RN2 (G1/G0) is 33%, RN3 (S) is 10.05% and RN4 (G2/M) is 7.40% respectively. Where as in formulation SD Figure 7B RN1(G1) is 12.746%, RN2 (G1/G0) is 43.30%, RN3 (S) is 12.04% and RN4 (G2/M) is 9.44% respectively. Dox arrested the cells in G1/G0 33 percentage whereas formulation SD proved better activity in G1/G0 phase with a percentage of 43.30. This shows formulation has better efficacy as compared to Dox.

DISCUSSION

Initially, the unique physicochemical properties of Dox and siRNA were harnessed to create sphingosomes by thin film hydration procedure. This method involved enclosing the drug within lipid bilayers, with siRNA being incorporated during the lipid membrane hydration process. Due to Dox's weakly basic nature, it entered the inner aqueous phase of the liposomes via active pH-gradient encapsulation, guaranteeing a high payload of the drug. The distribution of weak bases across lipid membranes was notably influenced by transmembrane pH gradients (ΔpH), underscoring the importance of precise pH control in the liposomal environment for optimal encapsulation efficacy.[44]

To achieve successful co-encapsulation, siRNA was initially actively encapsulated, followed by Dox loading. The entrapment efficiency of the sphingosomes exceeded 75.86%, as detailed in Table 1, validating the effectiveness of the adjustments made in sphingosome preparation.

In addition to achieving high entrapment efficiency, ideal liposomes should also display favorable attributes such as a small uniform size distribution, particle size and specific zeta potential. Among these characteristics, particle size plays a crucial role in determining the biological behavior of carriers. Larger particle sizes tend to reduce cell permeability and uptake, altering tissue distribution and making them more prone to immune system recognition and clearance, thus hindering passive targeting.[45-48] However, for sphingosomes encapsulating Dox and siRNA, their formulation tends to exhibit high delivery efficiency and accumulation in tumor tissues via the Permeability and Retention (EPR) effect.[49,50] The findings suggest that liposomes prepared using thin film hydration method demonstrated a desirable size of 165.1 nm.[51]

Zeta potential serves as another critical factor influencing the biological destiny of particles, impacting cellular adhesion/uptake and drug delivery. Typically, liposomes containing cationic lipids demonstrate heightened cell binding in comparison to those with anionic lipids due to electrostatic interaction with negatively charged cell membranes.[52] Given that DOX carries a positive charge, it was encapsulated within the internal phase of the liposomes, leaving the zeta potential of the sphingosomes unaffected, measured at -33.4 mV. The Polydispersity Index (PDI) of the formulation was determined to be 0.255, indicating good result quality. The augmented electrostatic repulsion between particles contributes to the stability of sphingosomes during storage and clinical application.[53]

Nanoparticle Tracking Analysis (NTA) determines particle size in a sample by analyzing the velocity of individual particles undergoing Brownian motion.[54] In traditional NTA, each particle's path is tracked across multiple images in a video generated by light scattering from the particles' movement over

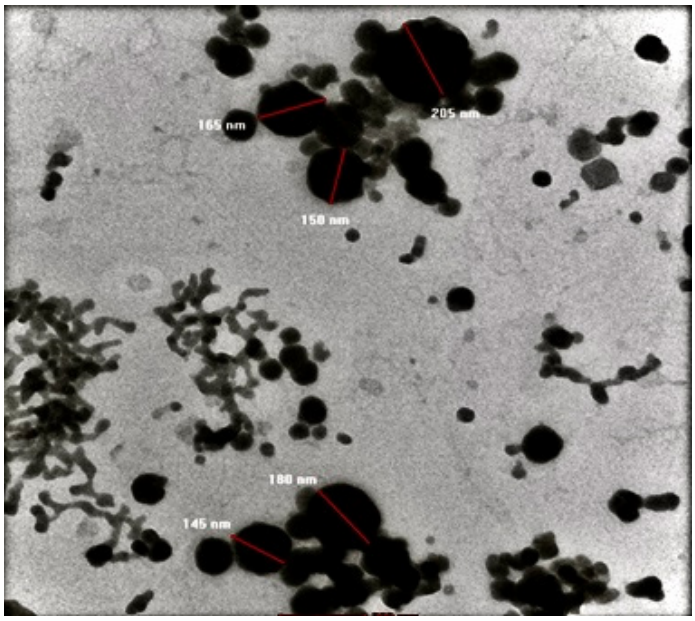

Figure 3: TEM image of the formulation SD.

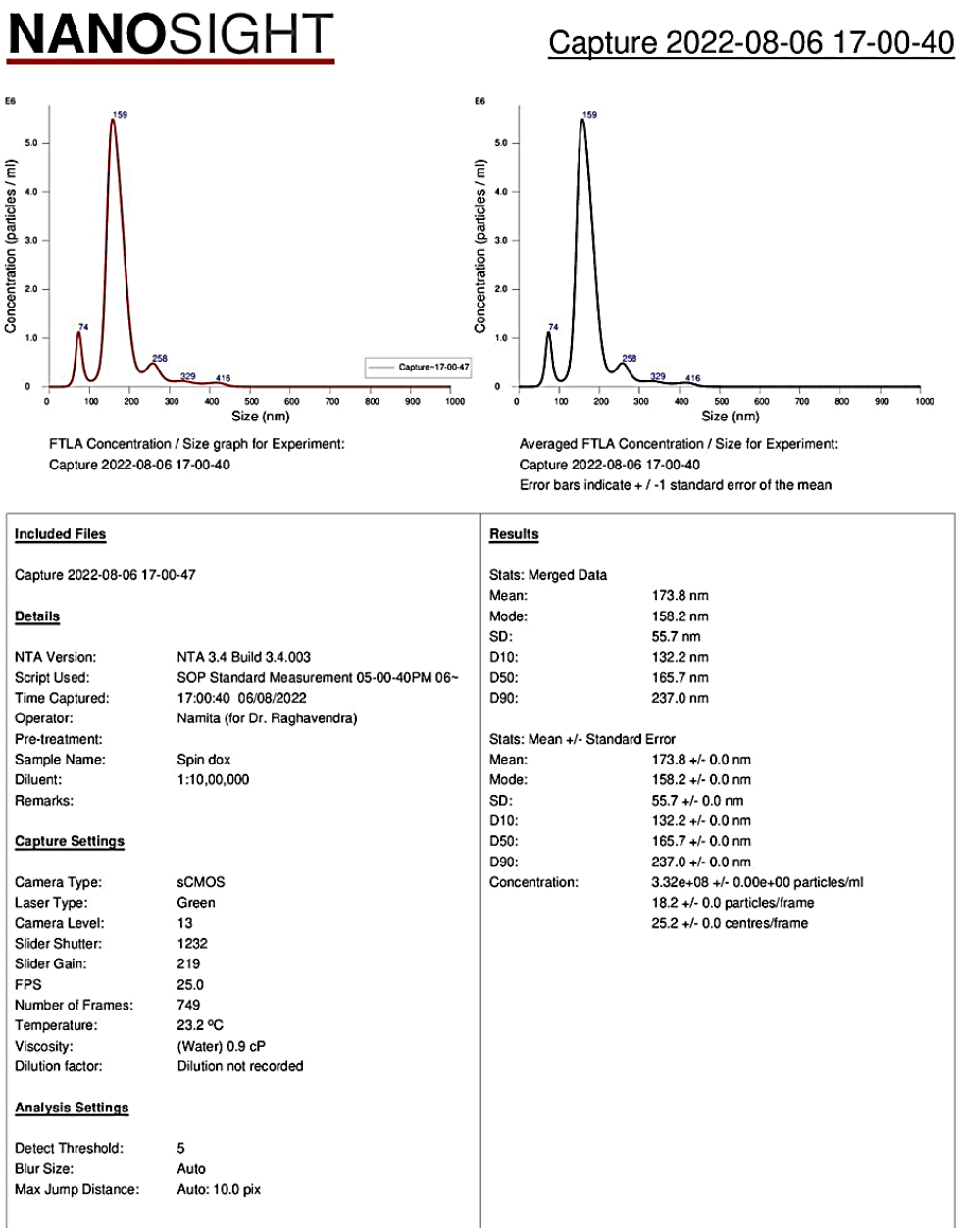

Figure 4: FTLA concentration/size graph for the formulation.

time. By assessing the mean squared distance traveled by a particle within a specific timeframe, the individual particle size is calculated. Nano Sight employs conventional NTA, utilizing a single laser to illuminate the sample volume and detecting the scattered light from freely diffusing particles. This technology has been effectively utilized for measuring particle size distribution ranging from 30 to 1000 nm.[55] For NTA analysis, Poly (Styrene) Latex (PSL) beads of sizes 70, 200, 600 and 1300 nm were utilized. Accurate particle size detection was achieved for individual PSLs and PSL mixtures up to 600 nm. Results presented in Figure 4 indicate a mean particle size of 173.8 nm, with D10, D50 and D90 values of 132.2 nm, 165.7 nm and 237.0 nm, respectively.

A decrease in the levels of the anti-apoptotic BCL2 protein triggers an increase in free pro-apoptotic Bax protein levels in the cytoplasm. This process facilitates the release of cytochrome C from the mitochondria, initiating the intrinsic pathway of apoptosis. The formulation lacking siRNA showed no toxicity to normal or cancerous cells. However, treatment with the siRNA Nano formulation resulted in decreased cell viability.

In our investigation using the MTT assay, free Dox exhibited an IC_{50} value of 0.621 µm, notably lower than that of sphingosomes, suggesting that Dox alone possesses high potency in inhibiting cell proliferation. Nonetheless, it's crucial to acknowledge that while free Dox may be more potent *in vitro*, its clinical utility can be limited by severe side effects, particularly cardiotoxicity. The higher IC_{50} of sphingosomes, though still effective, may reflect a more controlled and targeted delivery of Dox, potentially reducing off-target effects. The most intriguing aspect of our findings is the

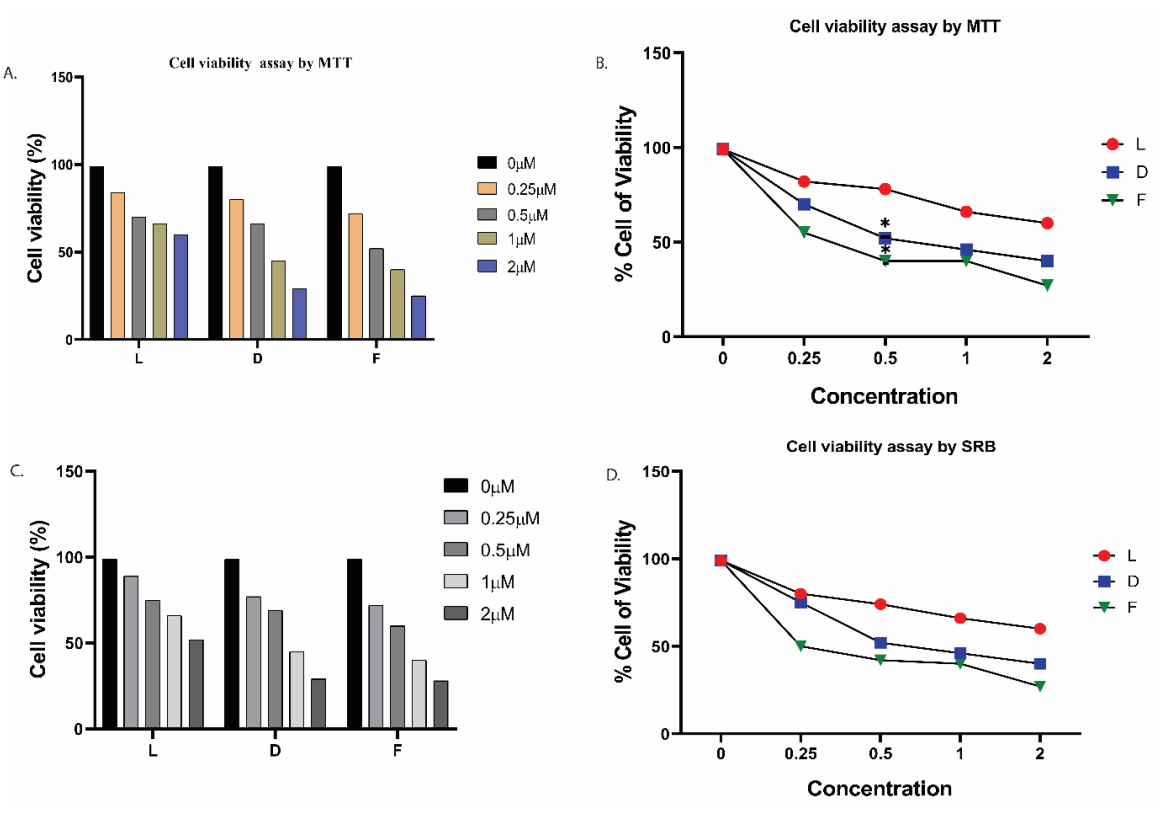

Figure 5: Assay of MTT (A and B) and SRB (C and D).

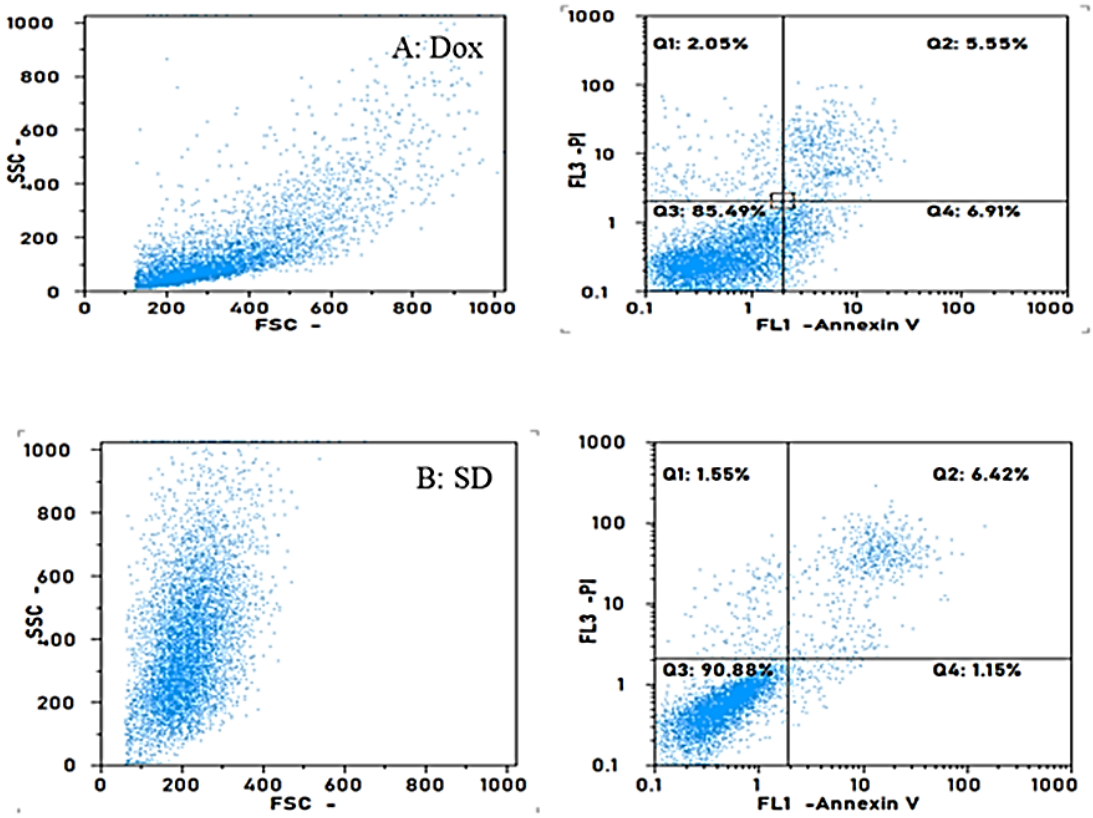

Figure 6: Apoptosis assay of A (Dox) and B (SD).

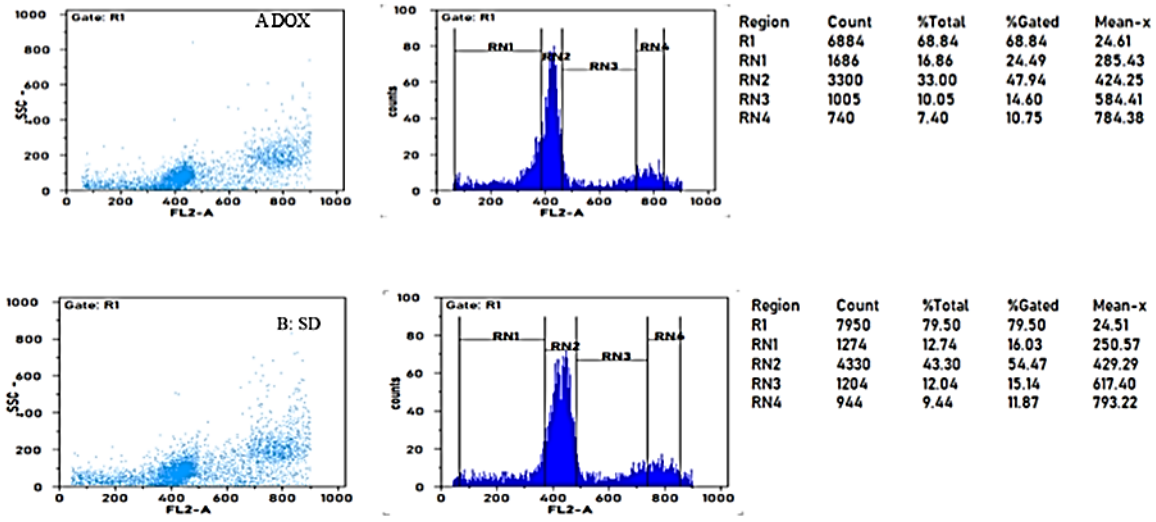

Figure 7: (A and B) Cell cycle analysis of Dox and SD formulation.

IC_{50} value of formulation SD, determined to be 0.285 µm. This result indicates that the Dox formulation SD is approximately twice as effective in inhibiting cell proliferation compared to free Dox. This observation underscores the crucial role of formulation in optimizing drug delivery. The finding that formulation SD is twice as effective as free Dox has significant clinical implications. By enhancing the drug's efficacy, formulation SD may allow for lower dosages of Dox, potentially reducing the risk of adverse side effects while maintaining therapeutic benefits. This is particularly important in cancer treatment, where balancing efficacy and safety is a constant challenge.

SRB assay results support the potential of sphingosomes as an effective drug delivery method for Dox, with controlled cytotoxicity compared to free Dox. Remarkably, formulation SD demonstrates remarkable efficacy, being twice as effective as free Dox in inhibiting cell proliferation. This finding holds promise for optimizing Dox delivery, potentially improving cancer treatment outcomes and reducing associated side effects.

The flow cytometry results depicted in Figure 6 A and B provide compelling evidence of the enhanced cellular uptake of Dox when formulated into sphingosomes, particularly in the presence of siRNA. In quadrant 3 of the scatter plot, where the fluorescence intensity of Dox is plotted against forward scatter, a distinct increase in Dox uptake is observed in the sphingosome formulation compared to Dox alone. Specifically, the percentage of cells exhibiting Dox uptake was found to be 85.49% in its standalone form, whereas in the formulation, it significantly escalated to 90.88%.

Quadrant 3, which represents cells with elevated Dox fluorescence intensity and forward scatter, corresponds to those with increased intracellular accumulation of the drug. The greater proportion of cells falling into this quadrant upon treatment with siRNA and Dox sphingosomes compared to Dox alone indicates more efficient uptake and retention of the drug within the tumor cells. This heightened cellular uptake can be attributed to the distinctive properties of sphingosomes, including their lipid-based composition and capacity to encapsulate drugs, thereby facilitating their effective delivery into cells.

Notably, controlling cell cycle progression in cancer cells is considered a potentially effective strategy for managing tumor growth.[56] Molecular analyses of human cancers have revealed frequent mutations in cell cycle regulators in most common malignancies.[57] Our data indicate that treating A549 cells with Dox and the SD formulation leads to significant G1-phase arrest of cell cycle progression, suggesting that one of the mechanisms by which they may inhibit cancer cell proliferation is by impeding cell cycle advancement.

The increased expression of G1 cyclins in cancer cells provides an unchecked growth advantage, as many of these cells either lack Cdk inhibitors or have insufficient levels of Cdk inhibitors to regulate Cdk-cyclin activity. G1-phase arrest of cell cycle progression offers cells an opportunity to undergo repair mechanisms or enter the apoptotic pathway.

CONCLUSION

In this work, an innovative co-delivery strategy using a sphingosomal formulation for lung cancer treatment was investigated. The formulation, termed SD formulation, was designed to simultaneously deliver BCL2 siRNA and Dox, a potent chemotherapy drug, to address the challenges of lung cancer treatment. Several key findings and conclusions can be drawn from this study:

Formulation Development

The sphingosomal formulation was meticulously developed using a combination of sphingomyelin and cholesterol, which provided stability and controlled release properties. This formulation allowed for the encapsulation of BCL2 siRNA and Dox within the lipid bilayer.

Characterization

The SD formulation exhibited favourable characteristics, including a small particle size (165.1 nm), a low polydispersity index (PDI) and a significant negative zeta potential (-33.4 mV). These attributes are crucial for efficient drug delivery systems.

Entrapment Efficiency

The formulation demonstrated high entrapment efficiency, with an impressive rate of 75.86%. This indicates that the encapsulation process for both BCL2 siRNA and Dox was successful.

Cytotoxicity Assays (MTT and SRB)

The study evaluated the cytotoxicity of the formulation against A549 lung cancer cells. In both MTT and SRB assays, the IC_{50} value for the SD formulation was significantly lower (0.285 µm in MTT and 0.357 µm in SRB) compared to free Dox (0.621 µm in MTT and 0.721 µm in SRB). This suggests that the SD formulation is approximately twice as effective in inhibiting cell proliferation compared to free Dox.

Flow cytometry results show the formulation is more effective compared to Dox alone which proves the formulation can be more effective in treatment of lung cancer with targeted delivery and minimizing side effects.

Based on the results presented in Figures 7A and 7B, it is evident that both Dox and the formulated SD exhibited significant effects on cell cycle progression. Specifically, Dox arrested cells predominantly in the G1/G0 phase at 33%, whereas the formulated SD demonstrated an even greater impact, with a higher percentage of 43.30% in the same phase. This suggests that the formulation SD has superior efficacy compared to Dox inducing cell cycle arrest, particularly in the G1/G0 phase. These findings highlight the potential of the formulated SD as a promising candidate for further development in cancer treatment strategies.

This finding represents a promising development in lung cancer treatment, addressing the delicate balance between treatment efficacy and patient safety.

CONCLUSION

In conclusion, the co-delivery strategy utilizing the sphingosomal formulation SD, carrying both BCL2 siRNA and Dox, shows remarkable potential for enhancing lung cancer treatment. The formulation's-controlled release properties, small particle size and significant cytotoxicity against cancer cells make it a promising candidate for further development. This study represents a significant step towards improving the effectiveness of lung cancer therapy while mitigating the associated side effects.

ACKNOWLEDGEMENT

The authors express their gratitude to NITTE (Deemed to be University) and NGSM Institute of Pharmaceutical Sciences for providing the essential laboratory facilities for conducting the research.

CONFLICT OF INTEREST

The authors declare that there is no conflict of interest.

FUNDING

The work is supported by NITTE (Deemed to be University) and NGSM Institute of Pharmaceutical Sciences.

ABBREVIATIONS

BCL2: B-cell Lymphoma 2; **SiRNA:** Small interfering RNA; **Dox:** Doxorubicin; **MTT:** (3-(4,5-dimethylthiazol-2-yl)-2,5-diphenyltetrazolium bromide; **SRB:** Sulforhodamine B; **IC_{50}:** Inhibitory concentration; **TEM:** Transmission electron microscopy; **NTA:** Nanoparticle Tracking Analysis; **A549:** Epithelial carcinoma of lungs; **SD:** Formulation Code; **PDI:** Polydispersity index; **EGFR:** Epidermal Growth Factor Receptor; **ALK:** Anaplastic Lymphoma Kinase; **SD:** Formulation code.

AUTHORS' CONTRIBUTIONS

R.N.C. oversaw the project's design, while P.N. authored the methodology. Formal analysis was carried out by R.N.C. and P.N., with validation of results conducted by both. R.N.C. and P.N. performed software analysis. Both authors contributed to the original draft preparation, final review and editing and approved the submitted version.

SUMMARY

The SD formulation, co-delivering BCL2 siRNA and Dox, shows considerable promise for lung cancer treatment. With controlled release, favorable particle characteristics and increased cytotoxicity, it presents itself as a strong candidate for further development. This co-delivery approach marks a significant step forward in enhancing the efficacy and safety of lung cancer therapies.

REFERENCES

1. Herlst RS, Heymach JV, Lippman SM. Molecular origins of cancer: lung cancer. New Engl J Med. 2008; 359: 1367-80.
2. Gottesman MM, Fojo T, Bates SE. Multidrug resistance in cancer: role of ATP–dependent transporters. Nature reviews cancer. 2002; 2(1): 48-58.
3. Citron ML, Berry DA, Cirrincione C, Hudis C, Winer EP, Gradishar WJ, Davidson NE, Martino S, Livingston R, Ingle JN, Perez EA. Randomized trial of dose-dense

versus conventionally scheduled and sequential versus concurrent combination chemotherapy as postoperative adjuvant treatment of node-positive primary breast cancer: first report of Intergroup Trial C9741/Cancer and Leukemia Group B Trial 9741. Journal of clinical oncology. 2003; 21(8): 1431-9. https:// doi. org/: 10.1200/J CO.2003.09.081

4. Yardley DA. Drug resistance and the role of combination chemotherapy in improving patient outcomes. International journal of breast cancer. 2013; 2013(1): 137414.
5. Dreicer R, Manola J, Roth BJ, See WA, Kuross S, Edelman MJ, Hudes GR, Wilding G. Phase III trial of methotrexate, vinblastine, doxorubicin, and cisplatin versus carboplatin and paclitaxel in patients with advanced carcinoma of the urothelium: a trial of the Eastern Cooperative Oncology Group. Cancer: Interdisciplinary International Journal of the American Cancer Society. 2004; 100(8): 1639-45. https: //doi.org/10.1002/cncr.20123
6. Du Bois A, Lück HJ, Meier W, Adams HP, Möbus V, Costa S, Bauknecht T, Richter B, Warm M, Schröder W, Olbricht S. A randomized clinical trial of cisplatin/paclitaxel versus carboplatin/paclitaxel as first-line treatment of ovarian cancer. Journal of the National Cancer Institute. 2003; 95(17): 1320-9. https://doi.org/10.1093/jnci/ djg 036
7. Pujade-Lauraine E, Wagner U, Aavall-Lundqvist E, Gebski V, Heywood M, Vasey PA, *et al*. Pegylated liposomal doxorubicin and carboplatin compared with paclitaxel and carboplatin for patients with platinum-sensitive ovarian cancer in late relapse. Journal of clinical oncology. 2010; 28(20): 3323-9. https:// doi. org/10.1200/JCO.20 09.25.7519
8. Chen AM, Zhang M, Wei D, Stueber D, Taratula O, Minko T, He H. Co-delivery of doxorubicin and BCL2 siRNA by mesoporous silica nanoparticles enhances the efficacy of chemotherapy in multidrug resistant cancer cells. Small (Weinheim an der Bergstrasse, Germany). 2009; 5(23): 2673. https:// doi. org/ 10.1002/ smll.20090 0621
9. Nardone G, Rocco A, Vaira D, Staibano S, Budillon A, Tatangelo F, Sciulli MG, Perna F, Salvatore G, Di Benedetto M, De Rosa G. Expression of COX-2, mPGE-synthase1, MDR-1 (P-gp), and Bcl-xL: a molecular pathway of H pylori-related gastric carcinogenesis. The Journal of pathology. 2004; 202(3): 305-12. https://doi.org/10. 1002/path.1512
10. Suo A, Qian J, Xu M, Xu W, Zhang Y, Yao Y. Folate-decorated PEGylated triblock copolymer as a pH/reduction dual-responsive nanovehicle for targeted intracellular co-delivery of doxorubicin and BCL2 siRNA. Materials Science and Engineering: C. 2017; 76: 659-72. https://doi.org/ 10.1016/j.msec. 2017 .03. 124
11. Feng T, Wei Y, Lee RJ, Zhao L. Liposomal curcumin and its application in cancer. International journal of nanomedicine. 2017: 6027-44. https://doi.org /10.2147 /IJN .S132434
12. Wang L, Xu X, Zhang Y, Zhang Y, Zhu Y, Shi J, Sun Y, Huang Q. Encapsulation of curcumin within poly (amidoamine) dendrimers for delivery to cancer cells. Journal of Materials Science: Materials in Medicine. 2013; 24: 2137-44. https:// doi. org/10.1007/ s10856-013-4969-3
13. Li Y, Lin Z, Zhao M, Xu T, Wang C, Xia H, Wang H, Zhu B. Multifunctional selenium nanoparticles as carriers of HSP70 siRNA to induce apoptosis of HepG2 cells. International journal of nanomedicine. 2016: 3065-76.
14. Xu Z, Wang D, Cheng Y, Yang M, Wu LP. Polyester based nanovehicles for siRNA delivery. Materials Science and Engineering: C. 2018; 92: 1006-15. https:// doi. org/ 10.1016/ j.msec. 2018. 05.
15. Büyükköroğlu G, Şenel B, Başaran E, Yenilmez E, Yazan Y. Preparation and in vitro evaluation of vaginal formulations including siRNA and paclitaxel-loaded SLNs for cervical cancer. European Journal of Pharmaceutics and Biopharmaceutics. 2016; 109: 174-83. https://doi.org/10.1016/j.ejpb.2016.10.017
16. Sun W, Chen X, Xie C, Wang Y, Lin L, Zhu K, Shuai X. Co-delivery of doxorubicin and anti-BCL2 siRNA by pH-responsive polymeric vector to overcome drug resistance in in vitro and in vivo HepG2 hepatoma model. Biomacromolecules. 2018; 19(6): 2248-56. https://doi.org/10.1021/acs.biomac.8b00272
17. Qian J, Xu M, Suo A, Xu W, Liu T, Liu X, Yao Y, Wang H. Folate-decorated hydrophilic three-arm star-block terpolymer as a novel nanovehicle for targeted co-delivery of doxorubicin and BCL2 siRNA in breast cancer therapy. Acta biomaterialia. 2015; 15: 102-16. https://doi.org /10.1016/ j.actbio. 2014. 12. 0 18.
18. Young SW, Stenzel M, Jia-Lin Y. Nanoparticle-siRNA: A potential cancer therapy?. Critical reviews in oncology/hematology. 2016; 98: 159-69. https://doi.org /10 .10 16 /j. critrevonc.2015.10.015
19. Abedi-Gaballu F, Dehghan G, Ghaffari M, Yekta R, Abbaspour-Ravasjani S, Baradaran B, Dolatabadi JE, Hamblin MR. PAMAM dendrimers as efficient drug and gene delivery nanosystems for cancer therapy. Applied materials today. 2018; 12: 177-90. Https: //doi .org/10.1016/j.apmt.2018.05.002
20. Wu D, Yang J, Xing Z, Han H, Wang T, Zhang A, Yang Y, Li Q. Phenylboronic acid-functionalized polyamidoamine-mediated BCL2 siRNA delivery for inhibiting the cell proliferation. Colloids and Surfaces B: Biointerfaces. 2016; 146: 318-25. https: // doi.org/ 10.1016 /j. colsurfb.2016.06.034
21. Li J, Liang H, Liu J, Wang Z. Poly (amidoamine)(PAMAM) dendrimer mediated delivery of drug and pDNA/siRNA for cancer therapy. International journal of pharmaceutics. 2018; 546(1-2): 215-25. https://doi.org/10.1016 /j.ijpharm .2018. 05. 045.
22. Abushouk AI, Ismail A, Salem AM, Afifi AM, Abdel-Daim MM. Cardioprotective mechanisms of phytochemicals against doxorubicin-induced cardiotoxicity. Biomedicine & Pharmacotherapy. 2017; 90: 935-46. https://doi.org/ 10.1016/ j. biopha. 2017. 04.033
23. Mobaraki M, Faraji A, Zare M, Dolati P, Ataei M, Manshadi HD. Molecular mechanisms of cardiotoxicity: a review on major side-effect of doxorubicin. Indian J Pharm Sci. 2017; 79(3): 335-44.
24. Gewirtz D. A critical evaluation of the mechanisms of action proposed for the antitumor effects of the anthracycline antibiotics adriamycin and daunorubicin. Biochemical pharmacology. 1999; 57(7): 727-41. https://doi.org /10.1016/ S0006-2952(98)00307-4
25. Box VG. The intercalation of DNA double helices with doxorubicin and nagalomycin. Journal of Molecular Graphics and Modelling. 2007; 26(1): 14-9. https://doi.org /10.1 016 /j.jmgm .2006. 09.005
26. Chatterjee K, Zhang J, Honbo N, Karliner JS. Doxorubicin cardiomyopathy. Cardiology. 2010; 115(2): 155-62. https://doi.org/10.1159/000265166.
27. Carvalho C, Santos RX, Cardoso S, Correia S, Oliveira PJ, Santos MS, Moreira PI. Doxorubicin: the good, the bad and the ugly effect. Current medicinal chemistry. 2009; 16(25): 3267-85. https://doi.org/10.2174/0929867097888033 1 2
28. Takemura G, Fujiwara H. Doxorubicin-induced cardiomyopathy: from the cardiotoxic mechanisms to management. Progress in cardiovascular diseases. 2007; 49(5): 330-52. https ://doi.org/10.1016/j.pcad.2006.10.002
29. Swain SM, Whaley FS, Ewer MS. Congestive heart failure in patients treated with doxorubicin: a retrospective analysis of three trials. Cancer: Interdisciplinary International Journal of the American Cancer Society. 2003; 97(11): 2869-79. https: //doi.org/ 10.1002/ cncr .11407
30. Von Hoff DD, Layard MW, Basa P, DAVIS Jr HL, Von Hoff AL, Rozencweig M, Muggia FM. Risk factors for doxorubicin-Induced congestive heart failure. Annals of internal medicine. 1979; 91(5): 710-7. https://doi.org/10.7326/0003-4819-91-5-710
31. Cirillo R, Sacco G, Venturella S, Brightwell J, Giachetti A, Manzini S. Comparison of doxorubicin-and MEN 10755-induced long-term progressive cardiotoxicity in the rat. Journal of cardiovascular pharmacology. 2000; 35(1): 100-8.
32. Wallace KB. Adriamycin-induced interference with cardiac mitochondrial calcium homeostasis. Cardiovascular toxicology. 2007; 7(2): 101-7. https://doi.org/10. 1007/s 12012-007-0008-2.
33. Nousiainen T, Jantunen E, Vanninen E, Remes J, Vuolteenaho O, Hartikainen J. Natriuretic peptides as markers of cardiotoxicity during doxorubicin treatment for non-Hodgkin's lymphoma. European journal of haematology. 1999; 62(2): 135-41. ht tps :// doi.org/ 10.1111/j.1600-0609. 1999.tb01734. x.
34. Gupta S, Kesarla R, Chotai N, Misra A, Omri A. Systematic approach for the formulation and optimization of solid lipid nanoparticles of efavirenz by high pressure homogenization using design of experiments for brain targeting and enhanced bioavailability. Biomed research international. 2017; 2017(1): 5984014. htt ps://doi.org/ 10.1155/2017/ 5984014.
35. Yasir M, Sara UV. Solid lipid nanoparticles for nose to brain delivery of haloperidol: in vitro drug release and pharmacokinetics evaluation. Acta Pharmaceutica Sinica B. 2014; 4(6): 454-63. https://doi.org/10.1016%20/j.apsb.2014.10.005
36. Anjum DH. Characterization of nanomaterials with transmission electron microscopy. InIOP Conference Series: Materials Science and Engineering 2016; 146(1): 012001. IOP Publishing. https://doi.org/ 10.1088/1757-899X/146/1/012001
37. Al-Ahmady ZS, Chaloin O, Kostarelos K. Monoclonal antibody-targeted, temperature-sensitive liposomes: *in vivo* tumor chemotherapeutics in combination with mild hyperthermia. Journal of Controlled Release. 2014; 196: 332-43. https://do i.org/10.1016/ j.jconrel. 2014. 10.013
38. Mosmann T. Rapid colorimetric assay for cellular growth and survival: application to proliferation and cytotoxicity assays. Journal of immunological methods. 1983; 65(1-2): 55-63. https://doi.org/10.1016/0022-1759(83)90303-4
39. Van Rensburg CJ, Anderson R, Jooné G, Myer MS, O'sullivan JF. Novel tetramethylpiperidine-substituted phenazines are potent inhibitors of P-glycoprotein activity in a multidrug resistant cancer cell line. Anti-cancer drugs. 1997; 8(7): 708-13. https:// doi .org/10.1097/00001813-199708000-00010
40. Stone V, Johnston H, Schins RP. Development of in vitro systems for nanotoxicology: methodological considerations. Critical reviews in toxicology. 2009; 39(7): 613-26. ht tps://doi.org/10.1080/10408440903120975
41. Kasinski AL, Kelnar K, Stahlhut C, Orellana E, Zhao J, Shimer E, Dysart S, Chen X, Bader AG, Slack FJ. A combinatorial microRNA therapeutics approach to suppressing non-small cell lung cancer. Oncogene. 2015; 34(27): 3547-55. https://doi.org /10.10 38 /onc. 2014. 282
42. Skehan P, Storeng R, Scudiero D, Monks A, McMahon J, Vistica D, Warren JT, Bokesch H, Kenney S, Boyd MR. New colorimetric cytotoxicity assay for anticancer-drug screening. JNCI: Journal of the National Cancer Institute. 1990; 82(13): 1107-12. https ://doi.org/ 10.1093 /jnci/ 82.13.1107
43. Vichai V, Kirtikara K. Sulforhodamine B colorimetric assay for cytotoxicity screening. Nature protocols. 2006; 1(3): 1112-6. https://doi.org/10.1038/ nprot. 2006. 179
44. Rehman AU, Omran Z, Anton H, Mély Y, Akram S, Vandamme TF, Anton N. Development of doxorubicin hydrochloride loaded pH-sensitive liposomes: Investigation on the impact of chemical nature of lipids and liposome composition on pH-sensitivity. European journal of pharmaceutics and biopharmaceutics. 2018; 133: 331-8. https://doi.org/10.1016/ j. ejpb.2018 .11.001
45. Ma S, Li M, Liu N, Li Y, Li Z, Yang Y, Yu F, Hu X, Liu C, Mei X. Vincristine liposomes with smaller particle size have stronger diffusion ability in tumor and improve tumor accumulation of vincristine significantly. Oncotarget. 2017; 8(50): 87276. https:// doi. org/10.18632/oncotarget.20162

46. Andar AU, Hood RR, Vreeland WN, DeVoe DL, Swaan PW. Microfluidic preparation of liposomes to determine particle size influence on cellular uptake mechanisms. Pharmaceutical research. 2014; 31: 401-13. https://doi.org/ 10.1007/s11095-013-1171-8
47. Chono S, Tauchi Y, Morimoto K. Influence of particle size on the distributions of liposomes to atherosclerotic lesions in mice. Drug development and industrial pharmacy. 2006; 32(1): 125-35. https://doi.org/ 10.1080/ 0363904050 0390645
48. Chu KS, Hasan W, Rawal S, Walsh MD, Enlow EM, Luft JC, Bridges AS, Kuijer JL, Napier ME, Zamboni WC, DeSimone JM. Plasma, tumor and tissue pharmacokinetics of Docetaxel delivered via nanoparticles of different sizes and shapes in mice bearing SKOV-3 human ovarian carcinoma xenograft. Nanomedicine: Nanotechnology, Biology and Medicine. 2013; 9(5): 686-93. https://doi.org/ 10.1016/ j.nano.2012.11.008
49. Maeda H. Toward a full understanding of the EPR effect in primary and metastatic tumors as well as issues related to its heterogeneity. Advanced drug delivery reviews. 2015; 91: 3-6. https://doi.org/10.1016/j.addr.2015.01.002
50. Wilhelm S, Tavares AJ, Dai Q, Ohta S, Audet J, Dvorak HF, Chan WC. Analysis of nanoparticle delivery to tumours. Nature reviews materials. 2016; 1(5): 1-2. https://doi.org/10.1038/natrevmats.2016.14
51. Soenen SJ, Brisson AR, De Cuyper M. Addressing the problem of cationic lipid-mediated toxicity: the magnetoliposome model. Biomaterials. 2009; 30(22): 3691-701. https://doi.org/ 10.1016/j. biomaterials .200 9. 03.040
52. Nie Y, Ji L, Ding H, Xie L, Li L, He B, Wu Y, Gu Z. Cholesterol derivatives based charged liposomes for doxorubicin delivery: preparation, *in vitro* and *in vivo* characterization. Theranostics. 2012; 2(11): 1092. https://doi.org/ 10. 7150 /thno.4949
53. Sainakham M, Manosroi A, Abe M, Manosroi W, Manosroi J. Potent *in vivo* anticancer activity and stability of liposomes encapsulated with semi-purified Job's tear (*Coix lacryma-jobi* Linn.) extracts on human colon adenocarcinoma (HT-29) xenografted mice. Drug delivery. 2016; 23(9): 3399-407.
54. Einstein A. Eine Theorie der Grundlagen der Thermodynamik. Annalen der Physik. 1903; 316(5): 170-87.
55. Filipe V, Hawe A, Jiskoot W. Critical evaluation of Nanoparticle Tracking Analysis (NTA) by NanoSight for the measurement of nanoparticles and protein aggregates. Pharmaceutical research. 2010; 27: 796-810. https://doi.org/ 10.1007/ s11095-010-007 3-2
56. Graña X, Reddy EP. Cell cycle control in mammalian cells: role of cyclins, cyclin dependent kinases (CDKs), growth suppressor genes and cyclin-dependent kinase inhibitors (CKIs). Oncogene. 1995; 11(2): 211-20.
57. Kastan MB, Canman CE, Leonard CJ. P53, cell cycle control and apoptosis: implications for cancer. Cancer and Metastasis reviews. 1995; 14: 3-15.

Cite this article: Nayak P, Charyulu RN. Co-Delivery of Sphingosomal Formulation Containing BCL2 siRNA Doxorubicin for the Treatment of Lung Cancer. Indian J of Pharmaceutical Education and Research. 2025;59(4):1293-304.